

Real-Time Registration of Volumetric Brain MRI by Biomechanical Simulation of Deformation during Image Guided Neurosurgery

Simon K. Warfield¹, Florin Talos^{1,2}, Alida Tei^{1,3}, Aditya Bharatha^{1,4}, Arya Nabavi^{1,2}, Matthieu Ferrant^{1,5}, Peter McL. Black², Ferenc A. Jolesz¹, Ron Kikinis¹

¹Surgical Planning Laboratory <http://www.spl.harvard.edu>, Department of Radiology, ²Department of Surgery, Brigham and Women's Hospital and Harvard Medical School, 75 Francis Street, Boston, MA 02115, ³Massachusetts Institute of Technology, Boston MA, ⁴University of Toronto Medical School, Toronto, Canada ⁵Telecommunications Laboratory, Université Catholique de Louvain, Belgium,

December 14, 2001.

Abstract. The key challenge faced by a neurosurgeon is the removal from the brain of as much tumor tissue as possible while minimizing the removal of healthy tissue and avoiding the disruption of critical anatomical structures. We developed an algorithm to create enhanced visualizations of tumor and critical brain structures by aligning preoperatively acquired image data with intraoperative images of the patient's brain during surgery.

To be practical for use during neurosurgery, the implementation must meet the real-time constraints of neurosurgery. We present here an analysis of the performance characteristics of an implementation of our algorithm on a high end symmetric multiprocessor architecture. We demonstrated that the implementation is sufficiently fast to be used during neurosurgery through scaling experiments and by using the algorithm to capture volumetric brain deformation during three neurosurgeries. The volumetric deformation is inferred through a biomechanical simulation with boundary conditions established via surface matching. We demonstrate the value of the enhanced visualization this algorithm allows.

Key words registration, image guided neurosurgery, high performance computing, volumetric biomechanical brain deformation model.

1 Introduction

The key challenge faced by a neurosurgeon is the removal from the brain of as much tumor tissue as possible while minimizing the removal of healthy tissue and avoiding the disruption of critical anatomical structures. This can be difficult because often healthy and diseased tissue have a similar visual appearance. Some critical structures, such as white matter fiber tracts, may not be visible at all.

Over the last decade the development of image guided surgery techniques has been a major advance in minimally invasive neurosurgery. These techniques, carried out in operating rooms equipped with special purpose imaging equipment,

Correspondence to: Simon K. Warfield, warfield@bwh.harvard.edu

allow the neurosurgeon to acquire new images during surgery. These images, such as provided by intraoperative ultrasound or intraoperative magnetic resonance imaging (IMRI), can provide improved contrast between healthy and diseased tissue, and the ability to see past the surface of the exposed brain in order to better appreciate the deeper structures of the brain. Due to the constraints of an operating room, intraoperative imaging typically results in images with lower signal to noise ratio and less flexibility in the choice of imaging modality than conventional imaging done outside the operating room.

We have developed an algorithm to allow the projection of preoperative images onto intraoperative images, allowing fusion of images from multiple imaging modalities and with multiple contrast types. The algorithm tracks surfaces of key structures in intraoperatively acquired images, allowing the projection of preoperative images into the configuration of the patient's brain during the neurosurgical procedure. A volumetric deformation field is inferred from the surface changes. This field captures nonrigid deformations of the shape of the brain due to factors such as brain swelling, cerebrospinal fluid loss, anaesthetic agents and the actions of the neurosurgeon. In order for this approach to have practical applicability during neurosurgery, it must meet the real-time constraints of neurosurgery. If the updated images arrive too late to provide meaningful guidance to the neurosurgeon then their value is lost.

We have carried out a performance assessment of a parallel implementation of our image registration algorithm. We evaluated the implementation on a high end symmetric multiprocessor architecture. This implementation is sufficiently fast to meet the constraints of neurosurgery. We can solve our biomechanical model inferring a three-dimensional volumetric deformation of the brain in less than ten seconds, and the entire image analysis process can be carried out in less than ten minutes. We used this implementation to track volumetric brain deformation during three neurosurgeries, and to project a preoperatively constructed model of the brain into the configuration of the patient's brain as its shape changed. We then constructed an enhanced visualization, merging preoperatively constructed surface models of the corticospinal tract from an anatomical atlas with intraoperative MRI and

surface models of the brain and ventricles of the patient and projected this visualization into the operating room.

1.1 Image Guided Neurosurgery

Image guided neurosurgery (IGNS) has largely been a visualization driven task. Quantitative assessment of intraoperative imaging data has not been possible in the past, and instead qualitative judgements by experts in the clinical domains have been relied upon. In order to provide the surgeon with as rich a visualization environment as possible from which to derive such judgements, previous work has primarily been concerned with image acquisition, visualization and registration of intraoperative and preoperative data. Biomechanically accurate registration of brain scans acquired during surgery, as proposed here, has the potential to be a significant aid to the automatic interpretation of intraoperative images and to enable prediction of surgical changes.

Early work, as described in the recent review by Jolesz [1], has established the importance and value of image guidance through the better localization of lesions, the better determination of tumor margins, and the optimization of the surgical approach. Previous algorithm development for computer aided IGNS has been a steady progression of improving image acquisition quality and speed, and more sophisticated and capable intraoperative image processing. Increasingly sophisticated multimodality image fusion and registration techniques have been developed. However, clinical experience with image guided therapy in deep brain structures and with large resections has revealed the limitations of existing rigid registration and visualization approaches [1]. This motivates the search for improved visualization technologies and for registration algorithms which can capture the nonrigid deformation of the brain during surgery.

Visualization during IGNS can be enhanced by preoperative images. Preoperative images can provide increased spatial resolution and contrast as compared to intraoperative images. Intraoperative imaging is by necessity limited in the time available for imaging and in the availability of different contrast mechanisms, whereas preoperative imaging is not limited in this way. A number of imaging modalities have been used for image guidance. These include, amongst others, digital subtraction angiography (DSA), computed tomography (CT), ultrasound (US), and magnetic resonance imaging (MRI). IMRI can acquire high contrast images of soft tissue anatomy which has proven to be very useful for image-guided therapy [2]. Multi-modality registration allows preoperative data that cannot be acquired intraoperatively, such as functional MRI (fMRI), nuclear medicine scans (such as Positron Emission Tomography (PET) and Single Photon Emission Computed Tomography (SPECT) scans) and magnetic resonance angiography (MRA) to be visualized together with intraoperative data.

A software system for intraoperative visualization has recently been developed [3]. This system allows surface rendering of previously prepared triangle models and arbitrary interactive resampling of 3D grayscale data. The system also allows for visualization of virtual surgical instruments in the coordinate system of the patient and patient image acquisitions. The system supports qualitative analysis based on ex-

pert inspection of the image data and the surgeons expectation of what should be present (normal anatomy, pathology, current progress of the surgery etc.)

The ability to automatically capture the deformation of the brain during neurosurgery as described in this work allows enhanced visualizations to be created by enabling surface models and cross-sectional data prepared preoperatively to be updated to follow the changes that occur during surgery. For example, this allows previously acquired functional MRI (which cannot be acquired intraoperatively) or diffusion tensor MRI to be transformed to place the preoperative scan in alignment with intraoperatively acquired morphologic MRI, facilitating more accurate interpretation based on the aligned preoperative information.

1.2 Nonrigid Registration in Support of IGNS

Over the course of a neurosurgery, the brain changes its shape in reaction to mechanical and physiological changes associated with the surgery. Suitable approaches to capture these shape changes and to create integrated visualizations of preoperative data in the configuration of the deformed brain are in active development. We categorize previous work aimed at capturing brain deformations for neurosurgery into those that use some form of biomechanical model (recent examples include [4–8]) and those that apply a phenomenological approach relying upon image related criteria (recent examples include [9–12].)

Purely image based matching is expected to be able to achieve a visually pleasing alignment, once issues of noise and intensity artifact rejection are accounted for. However, in our work for intraoperative matching we have favoured physics-based models which ultimately may be expanded to incorporate important inhomogeneous and anisotropic material characteristics of the brain.

In the domain of physics-based models, a spectrum ranging from less physically plausible but very fast models through to extremely accurate biomechanical models requiring hours of compute time to solve have been investigated.

A fast surgery simulation method was described in [13] which achieved speed by converting a volumetric finite element model into a model with only surface nodes. This work had the goal of achieving interactive graphics speeds at the cost of accuracy of the simulation. Such a model is applicable for computer graphics oriented visualization tasks such as surgical simulation where video frame rate results are required. However, during neurosurgical interventions on patients, our focus has been to aim for robustness and high accuracy in the matching, and we have used parallel hardware, parallel algorithm design and efficient parallel implementations of these algorithms in order to achieve execution times compatible with neurosurgery.

A sophisticated biomechanical model for two-dimensional brain deformation simulation using a finite element discretization was proposed in [4]. However this work established correspondences by manual interaction, and for the elements of the finite element discretization used the pixels of the two-dimensional image. Manually determining correspondences is susceptible to operator error and can be time consuming, especially when the generalization to deal with volumetric or

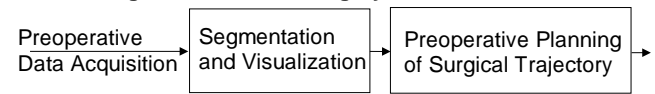
3D anatomy is attempted. Unfortunately two-dimensional results are not useful in clinical neurosurgical practice. A voxelwise discretization approach is extremely computationally expensive (even considering a parallel implementation) if expanded to three spatial dimensions because of the large number of voxels in a typical intraoperative MRI leading to a large number of equations to solve ($256 \times 256 \times 60 = 3,932,160$ voxels, which implies 11,796,480 displacements to determine). Downsampling can lead to fewer voxels, but leads to a crude approximation to the true geometry of interesting structures. Our approach is to construct an unstructured grid representing the geometry of the key structures, which allows us to use a finite element discretization that faithfully models key characteristics in important regions while reducing the number of equations to solve by using mesh elements that cover several image pixels in other regions.

Edwards et al. [14] presented a two dimensional three component model with the goal of tracking intraoperative deformation. This work used a simplified material model with the goal of achieving higher speed. The initial multigrid implementation on 2D images of 128×128 pixels converged to a solution in 120–180 minutes when run on a Sun Microsystems Sparc 20.

Skrinjar et al. [5] presented a very interesting system for real-time intraoperative brain shift capture for epilepsy neurosurgery where brain shift is rather slow. Brain surface points were tracked to indicate surface displacement. A simplified homogeneous brain tissue material model - a Kelvin solid model - was adopted since “it is a rather simple approach, which is a desirable property since the model deformation should be computed in real time . . . since it must be utilized during the surgery.” Their numerical model has 2088 nodes, 11733 connections and 1521 brick elements, and required “typically less than 10 minutes” on an SGI Octane R10000 workstation with one 250MHz processor. They conclude from these timings that “this model can potentially be used during the surgery, which is our eventual goal”. Following the description of surface based tracking from IMRI driving a linear elastic biomechanical model in [8], Skrinjar et al. presented a new implementation [7] of their system using a linear elastic model and surface based tracking from IMRI with the goal of eventually using stereoscopic cameras to obtain intraoperative surface data and hence to capture intraoperative brain deformation.

Paulsen et al. [15] and Miga et al. [6, 16] have developed a sophisticated finite element model to simulate brain deformation, incorporating simulations of forces associated with tumor tissue, and simulations of retraction and resection forces. Application of these models clinically will be very interesting as soon as intraoperative measurement of surgical instrument position and associated forces (such as pressure applied by the surgeon with the retractor) becomes possible. A limitation of their existing approach is that their preoperative segmentation and tetrahedral finite element mesh generation currently requires around five hours of operator time. They report post-operative simulation using a mesh of approximately 23200 nodes and 123500 elements (leading to roughly 92800 equations in their model) requiring 2 minutes for FEM loading, 8.5 minutes to simulate sag associated with gravitational force, 6.5 minutes to simulate resection, 5.5 minutes to simulate

Before Image Guided Neurosurgery:



During Image Guided Neurosurgery:

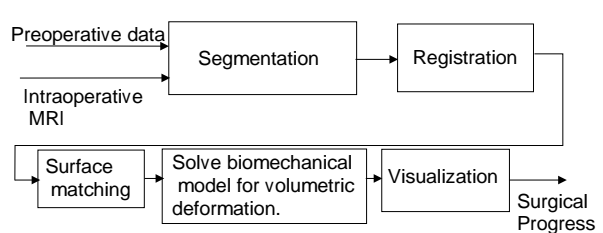


Fig. 1. Algorithm for enhanced visualization by projection of preoperative data into the intraoperative configuration of the subject’s anatomy.

excision and 6.0 minutes to simulate unretraction [16]. The hardware platform for these simulations was not reported.

For prediction of brain deformation, rather than capture of brain deformation from IMRI, a more sophisticated model of brain material properties would be required. Miller et al. [17, 18] have carried out pioneering simulations and comparisons with in vivo data to demonstrate that a hyper-viscoelastic constitutive model can reliably predict in vivo brain deformation induced by a force applied with constant loading velocity.

1.3 Summary

IGNS has become established as an important and effective surgical paradigm. Existing navigation algorithms are limited in their capability to capture brain deformation during surgery. In this study we aimed to demonstrate that a volumetric three-dimensional biomechanical simulation of brain deformation is possible even with the time constraints of neurosurgery and that such simulations significantly add to the value of intraoperative imaging and hence improve surgical outcomes.

2 Method

Figure 1 provides an overview of the image analysis steps that take place before and during the therapy procedure. The primary analysis tasks involve image segmentation and registration. Image segmentation is the process of identifying anatomical structures in volumetric imaging data. We exploit preoperative data acquisitions and preoperative segmentations for both preoperative planning of the surgical approach and to help create intraoperative segmentations as described below. Image registration in order to align the acquisitions involves both affine registration (to capture translation, rotation and scaling differences) and a biomechanical simulation of brain deformation.

The volumetric deformation is inferred through a biomechanical simulation with boundary conditions established via surface matching. Two major contributions of this paper are the demonstration that this sophisticated deformation model can be initialized and solved during a neurosurgery, and the demonstration of the value of the enhanced visualization this allows.

2.1 Preoperative Data Acquisition, Image Segmentation and Fusion

Since the time during surgery is limited compared to that available before surgery, preoperative data acquisition can be far more comprehensive than intraoperative data acquisition. The time available also allows a more extensive segmentation to be carried out.

Preoperative data can be segmented with a variety of manual [19], semi-automated [20,21] or automated [22–24] approaches and we select the most accurate, robust approach based upon the type of preoperative data and the particular critical structures.

For the matching experiments described below, we have made use of an anatomical atlas constructed from a high resolution MRI of a single subject. Over 200 anatomical structures have been segmented [25] using a combination of automated and interactive techniques. We are primarily interested in the corticospinal tract, a region of white matter which can be difficult or impossible to directly observe with conventional MRI. We have previously shown that we can project the corticospinal tract from the atlas onto patient scans for preoperative surgical planning [26].

2.2 Intraoperative Image Processing

Intraoperative image processing consists of acquiring a new intraoperative acquisition of one or more volumetric data sets, constructing a segmentation of the intraoperative acquisition, computing an affine registration of the preoperative data to the new acquisition, identifying the correspondences between key surfaces of the preoperative and intraoperative data, solving a biomechanical model to infer a volumetric deformation field, applying the deformation to the preoperative data and constructing a new visualization merging critical structures from the preoperative data with the intraoperative data.

2.2.1 Segmentation of Intraoperative Volumetric Images

In the experiments conducted below, a rapid segmentation of the brain was obtained through a binary curvature driven evolution algorithm [21]. The region identified as brain was then interactively corrected to remove any portion of misclassified skin and muscle using the software described by Gering et al. [3]. This was then repeated to obtain a segmentation of the lateral ventricles of the subject. This approach allows the neurosurgeon to inspect the segmentations as they are constructed during the surgery and enhances the surgeons confidence in the quality and availability of the segmentations.

We have also experimented with automated intraoperative segmentation [27,22] utilizing tissue classification in a multi-channel feature space with a model of expected anatomy. It is our expectation that this automated approach will be preferable once sufficient validation experiments have been carried out.

2.3 Unstructured Mesh Creation and Surface Representation

From the preoperative segmentation, we extract an explicit representation of the surface of the brain and ventricles. We also create a volumetric unstructured tetrahedral mesh representing the domain over which our biomechanical simulation of deformation will ultimately be executed. We generate a tetrahedral mesh of the brain and ventricles from segmentations of each volumetric intraoperative acquisition carried out during the surgery.

We have implemented a tetrahedral mesh generator specifically suited for labeled 3D medical images, building upon previously described techniques [28,29]. The mesh generator can be seen as the volumetric counterpart of a marching tetrahedra surface generation algorithm. A detailed description of the algorithm can be found in [11,30,31]. We can readily associate different biomechanical model parameters with different anatomical structures since the preoperative segmentation and tetrahedral mesh nodes have the same coordinate system.

2.3.1 Affine Registration of Preoperative Volumetric Images to Intraoperative Volumetric Images

For affine registration we use a fast and parallel implementation of an extremely robust algorithm which is based upon aligning segmented image data [32]. We register the brain segmentations of the preoperative and intraoperative scans. This allows us to capture affine transformation changes (rotation, translation and scaling) between the preoperative data and the subject scan.

2.3.2 Volumetric Biomechanical Simulation of Brain Deformation

As neurosurgery progresses the brain shape changes due to the surgical intervention (craniotomy, tissue resection, cerebrospinal fluid drainage are some of the factors). During IGNS the surgeon acquires a new volumetric MRI when he wishes to review the current configuration of the entire brain. A volumetric deformation field relating earlier acquisitions to this new scan is computed by first matching surfaces from the earlier acquisition to the new acquisition, and then inferring the volumetric deformation based upon the surface correspondences. The primary concept is to apply forces to the volumetric model that will produce the same displacement field at the surface as was obtained by the surface matching. The biomechanical model then allows the computation of the deformation throughout the volume.

Measuring Surface Correspondences An active surface algorithm iteratively deforms surfaces of both the brain and the lateral ventricles from the earlier acquisition to match that of the current acquisition. This is done iteratively by applying forces derived from the volumetric data to an elastic membrane model of the surface. The derived forces are a decreasing function of the image intensity gradients, so as to be minimized at the edges of objects in the volume. To increase robustness and the convergence rate of the process, we have included prior knowledge about the expected gray level and gradients of the objects being matched. This algorithm is fully described in [33, 34].

Biomechanical Simulation of Volumetric Brain Deformation We treat the brain as an homogeneous linear elastic material. The deformation energy of an elastic body, under no initial stresses or strains, subject to externally applied forces can be described by the following model [35]:

$$\mathbf{E} = \frac{1}{2} \int_{\Omega} \boldsymbol{\sigma}^T \boldsymbol{\varepsilon} \, d\Omega + \int_{\Omega} \mathbf{F}^T \mathbf{u} \, d\Omega \quad (1)$$

where $\mathbf{F} = \mathbf{F}(x, y, z)$ is the vector representing the forces applied to the elastic body (forces per unit volume, surface forces or forces concentrated at the nodes of the mesh), $\mathbf{u} = \mathbf{u}(x, y, z)$ the displacement vector field we wish to compute, and Ω the body on which one is working described by a mesh of tetrahedral elements. $\boldsymbol{\varepsilon}$ is the strain vector and $\boldsymbol{\sigma}$ the stress vector, linked to the strain vector by the constitutive equations of the material. For the above model, this relation is described as

$$\boldsymbol{\sigma} = (\sigma_x, \sigma_y, \sigma_z, \tau_{xy}, \tau_{yz}, \tau_{xz})^T = \mathbf{D}\boldsymbol{\varepsilon},$$

where \mathbf{D} is the elasticity matrix characterizing the material's properties [35]. Strain is related to displacement by the assumption $\boldsymbol{\varepsilon} = \mathbf{L}^T \mathbf{u}$ where \mathbf{L} is a linear operator.

A finite element discretization is used to obtain a mesh over the volumetric image domain. The mesh elements we use to represent volumetric data are tetrahedral and hence each element is defined by four mesh nodes. The continuous displacement field \mathbf{u} everywhere within element e of the mesh is defined as a function of the displacement at the element's nodes \mathbf{u}_i^e weighted by the element's interpolating functions $N_i^e(\mathbf{x})$,

$$\mathbf{u}(\mathbf{x}) = \sum_{i=1}^{N_{nodes}} \mathbf{I}N_i^e(\mathbf{x}) \mathbf{u}_i^e \quad (2)$$

We use linear interpolating functions to define the displacement field inside each element. Hence, the interpolating function of node i of tetrahedral element e is defined as

$$N_i^e(\mathbf{x}) = \frac{1}{6V_e} (a_i^e + b_i^e x + c_i^e y + d_i^e z) \quad (3)$$

The computation of the volume of the element V^e and the interpolation coefficients are detailed in [35, pages 91–92].

The volumetric deformation of the brain is found by solving for the displacement field that minimizes the energy described by Equation 1. Defining matrix $\mathbf{B}_i^e = \mathbf{L}N_i^e$ for every node i of each element e , solving for

$$\frac{\partial E(\mathbf{u}_1^e, \dots, \mathbf{u}_{N_{nodes}}^e)}{\partial \mathbf{u}_i^e} = 0 \quad ; \quad i = 1, \dots, N_{nodes} \quad (4)$$

yields the following equation :

$$\int_{\Omega} \sum_{j=1}^{N_{nodes}} \mathbf{B}_i^{eT} \mathbf{D} \mathbf{B}_j^e \mathbf{u}_j^e \, d\Omega = - \int_{\Omega} \mathbf{F} N_i^e \, d\Omega \quad ; \quad i = 1, \dots, N_{nodes}. \quad (5)$$

This can be written as a linear equation system, which can be solved for the displacements resulting from the forces applied to the body :

$$\mathbf{K} \mathbf{u} = -\mathbf{F}. \quad (6)$$

The displacements at the boundary surface nodes are fixed to match those generated by the active surface model. Let $\tilde{\mathbf{u}}$ be the vector representing the displacement to be imposed at the boundary nodes. The elements of the rows of the stiffness matrix \mathbf{K} corresponding to the nodes for which a displacement is to be imposed are set to zero and the diagonal elements of these rows to one. The force vector \mathbf{F} is set to equal the displacement vector for the boundary nodes: $\mathbf{F} = \tilde{\mathbf{u}}$ [35]. In this way solving Equation 6 for the unknown displacements will produce a deformation field over the entire mesh that matches the prescribed displacements at the boundary surfaces.

2.4 Hardware for Intraoperative Image Acquisition and Parallel Computation

The volumetric deformation of the brain is found by solving for the displacement field that minimizes the energy described by Equation 1, after fixing the displacements at the surface to match those generated by the active surface model.

At each node of the finite element mesh, three variables representing the x,y and z displacements are to be determined. Each variable gives rise to one row and one column in the global \mathbf{K} matrix. The rows of the matrix are divided equally amongst the CPUs available for computation and the global matrix is assembled in parallel. Each CPU assembles the local \mathbf{K}^e matrix for each element in its subdomain. Each CPU has an equal number of rows to process but because the connectivity of the mesh is irregular, some CPUs may do more work than other CPUs.

Following the assembly of the matrix, the boundary conditions determined by the surface matching are applied. The global \mathbf{K} matrix is adjusted such that rows associated with variables that are determined consist of a single non-zero entry of unit magnitude on the diagonal.

We solve the volumetric biomechanical brain model system of equations (and the active surface membrane model equations) with the Portable, Extensible Toolkit for Scientific Computation (PETSc) package [36, 37] using the Generalized Minimal Residual (GMRES) solver with block Jacobi preconditioning. During neurosurgery, the system of equations was solved on a Sun Microsystems SunFire 6800 symmetric multi-processor machine with 12 750MHz UltraSPARC-III (8MB Ecache) CPUs and 12 GB of RAM. This architecture gives us sufficient compute capacity to execute the intraoperative image processing during a neurosurgery.

Figure 2 shows the open-configuration magnetic resonance scanner optimized for imaging during surgical procedures [1, 2]. The image we constructed is presented on the LCD and increases the information available to the surgeon as the operation progresses.

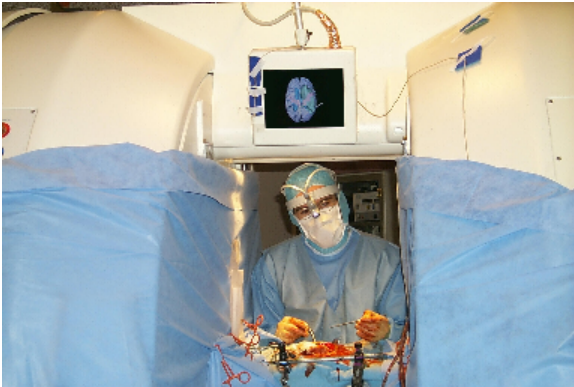


Fig. 2. Neurosurgeon standing inside the intraoperative magnetic resonance imaging scanner in which image guided therapy takes place. The operating room consists entirely of equipment safe to use around a 0.5T magnetic field. The surgeon operates on the exposed brain of the patient seen lying on the bed, and the enhanced visualization is displayed on the LCDs immediately above the surgeon (one on each side of the magnet bore). The LCD displays the intraoperative MRI, surface rendering of the tumor and lateral ventricles from segmentations of the intraoperative MRI and the corticospinal tract projected from an anatomical atlas onto the patient intraoperative MRI.

2.5 Augmented Visualization

Once the volumetric deformation field has been obtained, we can apply this to earlier data to warp it into the current configuration of the patient's brain. We can project both imaging data, such as preoperative MRI or nuclear medicine scans, and segmentations. We display the imaging data by texture mapping onto flat planes. This allows ready comparison of the current intraoperative scan and earlier scans. We construct new triangle models to enable surface rendering of segmented structures in 3D. This allows ready appreciation of the 3D anatomy of these segmented structures together with the imaging data in the form of planes passing through or over the 3D triangle models [3].

These visualizations are rendered on a Sun Microsystems workstation with hardware accelerated triangle rendering and texture mapping and displayed on LCD screens attached to the open magnet MRI scanner. The surgeon can then visualize directly the surface of the patient's brain, the volumetric representation of the internal structure of the brain from IMRI augmented with earlier image acquisitions, and 3D surface models of selected structures in the correct alignment. This augments the surgeon's ability to see critical structures which must be preserved (such as the corticospinal tract) and to better appreciate the tumor and its relationship to these critical structures.

3 Results

We present visualizations derived from intraoperative magnetic resonance images acquired during surgery in order to indicate the accuracy of the image analysis algorithm in capturing intraoperative brain deformations.

Enhancement of the intraoperative visualization enabled by this algorithm is illustrated by matching the corticospinal

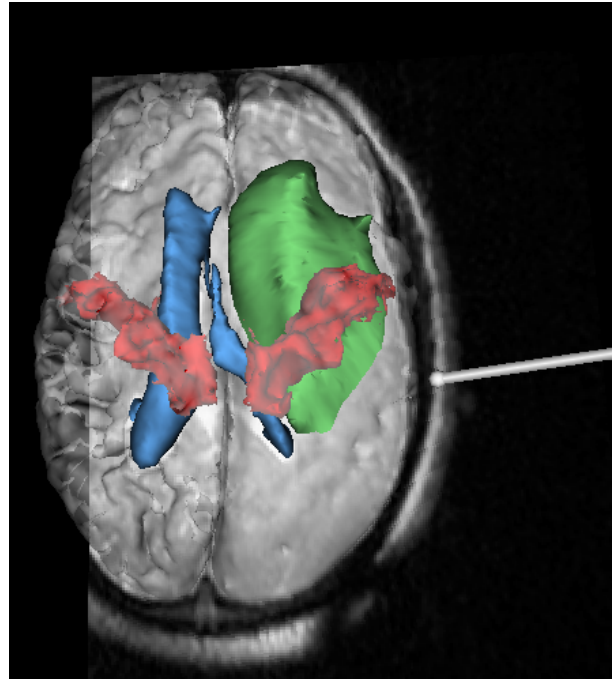


Fig. 3. This figure shows the corticospinal tract from our anatomical atlas in red, projected into the shape of the brain of the subject shown in Figure 2. The tumor is shown in green, the lateral ventricles in blue, and the brain derived from an IMRI earlier in the surgery is rendered in gray. A real-time 2D IMRI image indicated by the pointer has just been acquired and is being visualized together with the models and previous acquisition in order to assess the current status of the neurosurgical progress.

tract of a preoperatively prepared anatomical atlas to an intraoperative scan of a subject. This matching was carried out during the neurosurgery, demonstrating the practical value of the approach and its ability to meet the real-time constraints of surgery.

A set of parallel scaling experiments were carried out to demonstrate the scaling characteristics of the parallel implementation of the algorithm. These experiments again show that we can meet the real-time constraints of surgery, and that even a relatively sophisticated biomechanical simulation of deformation can be solved sufficiently rapidly for use during surgery.

We present illustrative results obtained by applying the image analysis described above during three neurosurgeries.

3.1 Biomechanical Simulation of Volumetric Brain Deformation

Figure 3 shows the corticospinal tract from our anatomical atlas projected into the shape of the brain of the subject shown in Figure 2. This visualization helps the surgeon to better understand the 3D relationship of the corticospinal tract, a critical white matter structure which should not be disrupted during surgery, and the rest of the brain. The corticospinal tract cannot be readily observed in IMRI acquisitions.

Figure 4 illustrates the amount of brain deformation which can occur during neurosurgery, as well as the ability of our

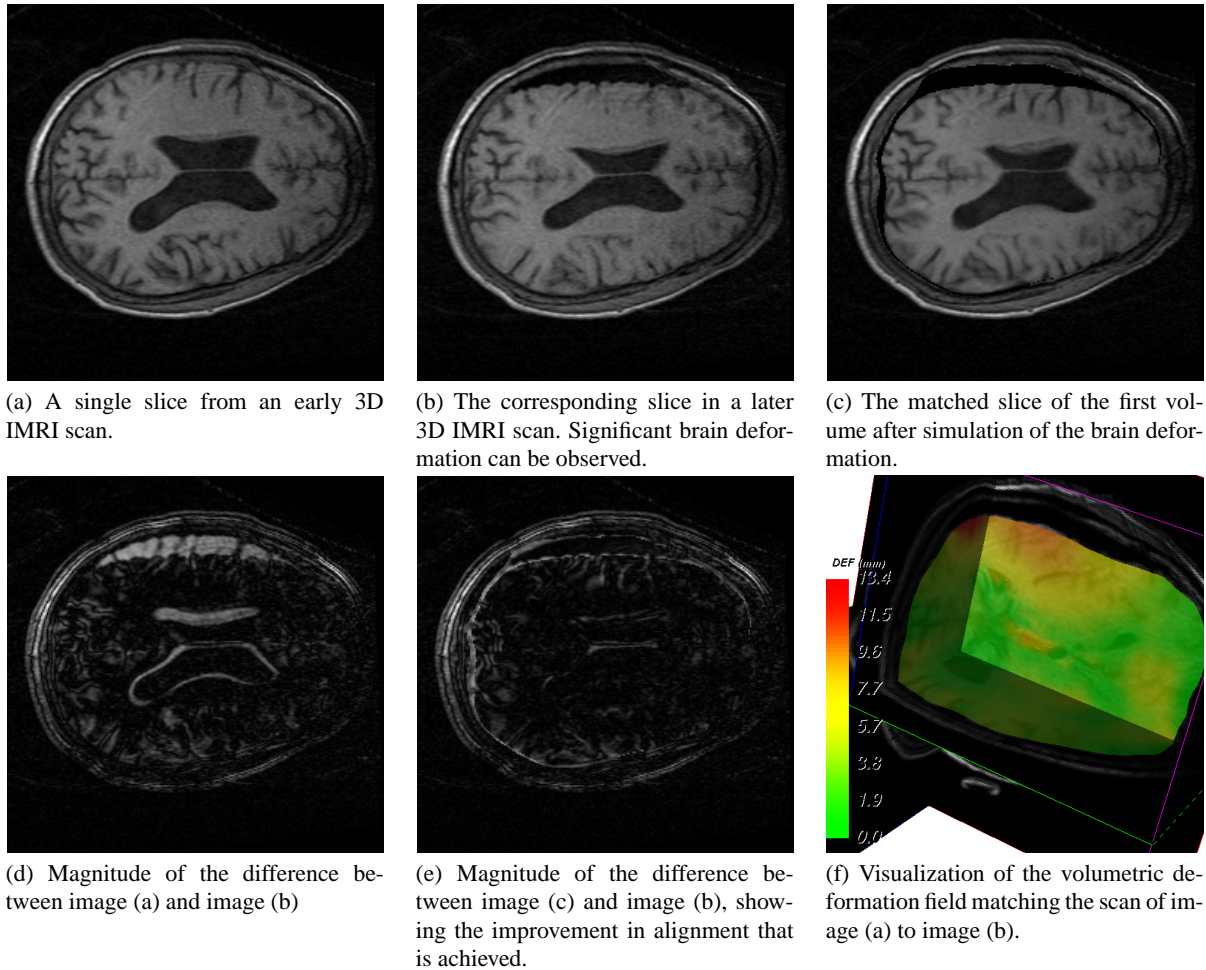


Fig. 4. Two dimensional slices through three-dimensional data, showing the match of the simulated deformation of the initial brain onto the actual deformed brain. The quality of the match is significantly better than can be obtained through rigid registration alone. The closeness of the match of the simulated deformation to the actual deformation can be judged by the very small intensity differences at the boundary of the simulated deformed brain and the air gap inside the skull of the target image. Some small intensity differences are expected because intrinsic MR scanner intensity variability causes a small variation in the observed voxel intensities from scan to scan.

algorithm to capture this shift during neurosurgery. The quality of the match is significantly better than can be obtained through rigid registration alone. The closeness of the match of the simulated deformation to the actual deformation can be judged by the very small intensity differences at the boundary of the simulated deformed brain and the air gap inside the skull of the target image. Some small intensity differences are expected because intrinsic MR scanner intensity variability causes a small variation in the observed voxel intensities from scan to scan.

3.2 Performance Analysis of Parallel Implementation

Ultimately, the utility of use these intraoperative image analysis methods relies upon them being sufficiently robust to provide accurate results (significantly better than the current best affine transformations) for typical clinical cases, and critically, to be sufficiently fast to provide feedback to the surgeon at a rate that is practical for routine use during neurosurgery.

In order to provide a context for the biomechanical simulation amongst the other image analysis and acquisition tasks

that must occur intraoperatively, typically timings we have observed for the intraoperative image analysis described here is shown in Figure 5. The most computationally demanding task, the biomechanical simulation, has been the focus of most optimization in our implementation, and is now the fastest component. The complete execution time for the intraoperative image analysis is less than ten minutes, and this has been adequate to display updated images to the neurosurgeon during three neurosurgeries. However, we expect it will be possible to further reduce this time, primarily by reducing the user interaction in the segmentation step.

Figure 6 illustrates the computation time required for the biomechanical model on a Sun Microsystems Sun Fire 6800 with 12 750MHz UltraSPARC-III CPUs. The figure shows that on a single CPU the parallel assembly of system of equations requires 17 seconds, the solution of the system of equations requires 37 seconds, and the overall solution time requires 57 seconds. The overall solution time is the sum of times for creation, initialization, assembly of the stiffness matrix, solution and force vectors, solving the system and gathering of the parallel result vector into a single sequential vec-

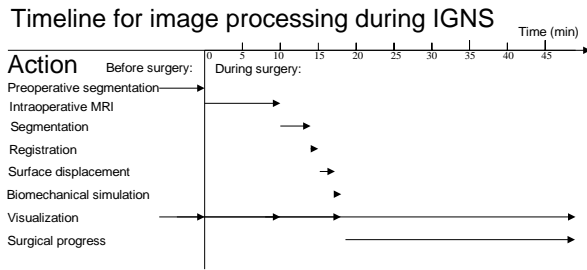


Fig. 5. Typical timings for image analysis events occurring before and during image guided neurosurgery.

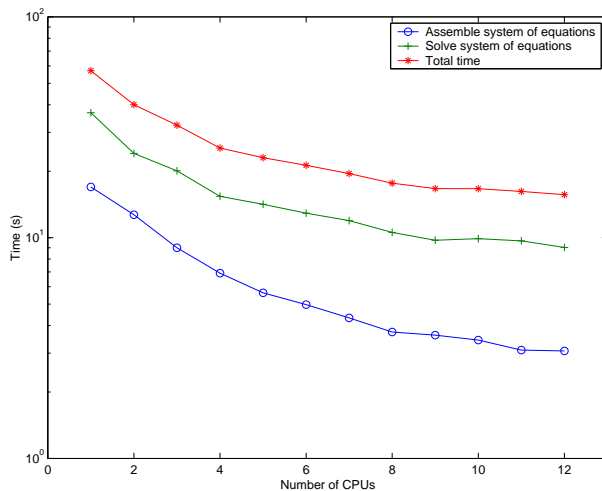


Fig. 6. Total computation time, time to assemble, and time to solve the biomechanical simulation of brain deformation for the neurosurgery case illustrated in Figure 2. The total number of mesh nodes was 43584, defining 214035 tetrahedral elements. This represents a system of $43584 \times 3 = 130752$ unknown displacements to be identified.

tor. Running on all 12 CPUs, the parallel assembly of system of equations requires 3 seconds, the solution of the system of equations requires 9 seconds, and the overall solution time requires 15 seconds, which is the sum of times for creation, initialization, assembly of the matrix and vectors, solving the system, scatter of the parallel result vector into a common sequential vector.

4 Discussion and Conclusion

Our early experience during three neurosurgery cases indicates that our intraoperative biomechanical simulation of brain deformation algorithm is a robust and reliable method for capturing the changes in brain shape that occur during neurosurgery. The registration algorithm requires no user interaction and the parallel implementation is sufficiently fast to be used intraoperatively.

Intraoperative registration adds significantly to the value of intraoperative imaging. It provides for quantitative monitoring of therapy application including the ability to make quantitative comparisons with a preoperatively determined treatment plan and enables preoperative data to be aligned

with the current configuration of the brain of the patient in order to allow 3D interactive visualization of fused multi-modality data.

In the future we intend to incorporate patient-specific preoperative data in place of the anatomical atlas we currently use. This will increase the surgical value of the intraoperative updates of preoperative data.

The parallel implementation described here could be improved by addressing the load imbalances in order to achieve better scaling performance. A tetrahedral mesh with a more regular connectivity pattern would allow better scaling in the matrix assembly process. The parallel decomposition of the system of equations to solve could be modified to account for the distribution of known displacements in order to improve the scaling of the solver.

Improved registration could result from a more sophisticated model of the material properties of the brain (such as more accurate modelling of the cerebral falx and the lateral ventricles). The creation of an intraoperative segmentation system able to identify these structures would be necessary to enable such a model to be applied routinely in surgery. Sophisticated MR imaging methods such as diffusion tensor MRI now enable the preoperative imaging of inhomogeneous anisotropic white matter structure. It would be interesting to incorporate a material model reflecting these structural characteristics of white matter.

Prediction of brain deformation, as opposed to the capture of observed deformation described here, will most likely require a nonlinear material model together with extensive monitoring of physiological data. Such prediction could be used to indicate when new intraoperative imaging is necessary to appropriately update both the simulation model and the surgeons understanding of the brain shape. It will be crucial to validate such predictions in a setting which reflects the actual neurosurgical environment and events as accurately as possible. Serial volumetric IMRI acquisitions obtained during neurosurgery will provide a critical test by allowing objective assessment of the accuracy of brain deformation prediction algorithms.

Acknowledgements. This investigation was supported by NIH grants P41 RR13218, P01 CA67165, R01 RR11747, R01 CA86879 and by a New Concept Award from the Center for Integration of Medicine and Innovative Technology (SKW).

References

1. F. Jolesz, "Image-guided Procedures and the Operating Room of the Future," *Radiology*, vol. 204, pp. 601–612, May 1997.
2. P. M. Black, T. Moriarty, E. Alexander, P. Stieg, E. J. Woodard, P. L. Gleason, C. H. Martin, R. Kikinis, R. B. Schwartz, and F. A. Jolesz, "The Development and Implementation of Intraoperative MRI and its Neurosurgical Applications," *Neurosurgery*, vol. 41, pp. 831–842, April 1997.
3. D. Gering, A. Nabavi, R. Kikinis, N. Hata, L. O'Donnell, W. Grimson, F. Jolesz, P. Black, and W. Wells III, "An integrated visualization system for surgical planning and guidance using image fusion and an open MR," *J Magn Reson Imaging*, vol. 13, pp. 967–975, Jun 2001.

4. A. Hagemann, K. Rohr, H. S. Stiel, U. Spetzger, and J. M. Gilsbach, "Biomechanical modeling of the human head for physically based, non-rigid image registration," *IEEE Transactions On Medical Imaging*, vol. 18, no. 10, pp. 875–884, 1999.
5. O. Skrinjar and J. S. Duncan, "Real time 3D brain shift compensation," in *IPMI'99*, pp. 641–649, 1999.
6. M. Miga, K. Paulsen, J. Lemery, A. Hartov, and D. Roberts, "In vivo quantification of a homogeneous brain deformation model for updating preoperative images during surgery," *IEEE Transactions On Medical Imaging*, vol. 47, pp. 266–273, February 1999.
7. O. Skrinjar, C. Studholme, A. Nabavi, and J. Duncan, "Steps Toward a Stereo-Camera-Guided Biomechanical Model for Brain Shift Compensation," in *Proceedings of International Conference of Information Processing in Medical Imaging*, pp. 183–189, 2001.
8. M. Ferrant, S. K. Warfield, A. Nabavi, B. Macq, and R. Kikinis, "Registration of 3D Intraoperative MR Images of the Brain Using a Finite Element Biomechanical Model," in *MICCAI 2000: Third International Conference on Medical Robotics, Imaging And Computer Assisted Surgery; 2000 Oct 11–14; Pittsburgh, USA* (A. M. DiGioia and S. Delp, eds.), (Heidelberg, Germany), pp. 19–28, Springer-Verlag, 2000.
9. D. Hill, C. Maurer, R. Maciunas, J. Barwise, J. Fitzpatrick, and M. Wang, "Measurement of intraoperative brain surface deformation under a craniotomy," *Neurosurgery*, vol. 43, pp. 514–526, 1998.
10. N. Hata, *Rigid and deformable medical image registration for image-guided surgery*. PhD thesis, University of Tokyo, 1998.
11. M. Ferrant, S. K. Warfield, C. R. G. Guttmann, R. V. Mulkern, F. A. Jolesz, and R. Kikinis, "3D Image Matching Using a Finite Element Based Elastic Deformation Model," in *MICCAI 99: Second International Conference on Medical Image Computing and Computer-Assisted Intervention; 1999 Sep 19–22; Cambridge, England* (C. Taylor and A. Colchester, eds.), (Heidelberg, Germany), pp. 202–209, Springer-Verlag, 1999.
12. N. Hata, A. Nabavi, W. M. Wells, S. K. Warfield, R. Kikinis, P. M. Black, and F. A. Jolesz, "Three-Dimensional Optical Flow Method for Measurement of Volumetric Brain Deformation from Intraoperative MR Images," *J Comput Assist Tomogr*, vol. 24, pp. 531–538, Jul-Aug 2000.
13. M. Bro-Nielsen, "Surgery Simulation Using Fast Finite Elements," in *Visualization in Biomedical Computing*, pp. 529–534, 1996.
14. P. J. Edwards, D. L. G. Hill, J. A. Little, and D. J. Hawkes, "Deformation for Image Guided Interventions Using a Three Component Tissue Model," in *IPMI'97*, pp. 218–231, 1997.
15. K. Paulsen, M. Miga, F. Kennedy, P. Hoopes, A. Hartov, and D. Roberts, "A Computational Model for Tracking Subsurface Tissue Deformation During Stereotactic Neurosurgery," *IEEE Transactions On Medical Imaging*, vol. 47, pp. 213–225, February 1999.
16. M. I. Miga, D. W. Roberts, F. E. Kennedy, L. A. Platenik, A. Hartov, K. E. Lunn, and K. D. Paulsen, "Modeling of Retraction and Resection for Intraoperative Updating of Images," *Neurosurgery*, vol. 49, pp. 75–85, July 2001.
17. K. Miller and K. Chinzei, "Constitutive modelling of brain tissue: experiment and theory," *J Biomech*, vol. 30, pp. 1115–1121, Nov–Dec 1997.
18. K. Miller, K. Chinzei, G. Orsengo, and P. Bednarz, "Mechanical properties of brain tissue in-vivo: experiment and computer simulation," *J Biomech*, vol. 33, pp. 1369–1376, Nov 2000.
19. D. Gering, A. Nabavi, R. Kikinis, W. Grimson, N. Hata, P. Everett, F. Jolesz, and W. Wells, "An Integrated Visualization System for Surgical Planning and Guidance using Image Fusion and Interventional Imaging," in *MICCAI 99: Proceedings of the Second International Conference on Medical Image Computing and Computer Assisted Intervention*, pp. 809–819, Springer Verlag, 1999.
20. R. Kikinis, M. E. Shenton, G. Gerig, J. Martin, M. Anderson, D. Metcalf, C. R. G. Guttmann, R. W. McCarley, W. E. Lorensen, H. Cline, and F. Jolesz, "Routine Quantitative Analysis of Brain and Cerebrospinal Fluid Spaces with MR Imaging," *Journal of Magnetic Resonance Imaging*, vol. 2, pp. 619–629, 1992.
21. A. Yezzi, A. Tsai, and A. Willsky, "Medical image segmentation via coupled curve evolution equations with global constraints," in *Mathematical Methods in Biomedical Image Analysis*, pp. 12–19, 2000.
22. S. K. Warfield, M. Kaus, F. A. Jolesz, and R. Kikinis, "Adaptive, Template Moderated, Spatially Varying Statistical Classification," *Med Image Anal*, vol. 4, pp. 43–55, Mar 2000.
23. M. R. Kaus, S. K. Warfield, A. Nabavi, E. Chatzidakis, P. M. Black, F. A. Jolesz, and R. Kikinis, "Segmentation of MRI of meningiomas and low grade gliomas," in *MICCAI 99: Second International Conference on Medical Image Computing and Computer-Assisted Intervention; 1999 Sep 19–22; Cambridge, England* (C. Taylor and A. Colchester, eds.), (Heidelberg, Germany), pp. 1–10, Springer-Verlag, 1999.
24. S. K. Warfield, R. V. Mulkern, C. S. Winalski, F. A. Jolesz, and R. Kikinis, "An Image Processing Strategy for the Quantification and Visualization of Exercise Induced Muscle MRI Signal Enhancement," *J Magn Reson Imaging*, vol. 11, pp. 525–531, May 2000.
25. R. Kikinis, M. E. Shenton, D. V. Iosifescu, R. W. McCarley, P. Saiviroonporn, H. H. Hokama, A. Robatino, D. Metcalf, C. G. Wible, C. M. Portas, R. M. Donnino, and F. A. Jolesz, "A Digital Brain Atlas for Surgical Planning, Model Driven Segmentation, and Teaching," *IEEE Transactions on Visualization and Computer Graphics*, vol. 2, pp. 232–241, September 1996.
26. M. R. Kaus, A. Nabavi, C. T. Marnisch, W. M. Wells, F. A. Jolesz, R. Kikinis, and S. K. Warfield, "Simulation of Corticospinal Tract Displacement in Patients with Brain Tumors," in *MICCAI 2000: Third International Conference on Medical Robotics, Imaging And Computer Assisted Surgery; 2000 Oct 11–14; Pittsburgh, USA* (A. M. DiGioia and S. Delp, eds.), (Heidelberg, Germany), pp. 9–18, Springer-Verlag, 2000.
27. S. K. Warfield, F. A. Jolesz, and R. Kikinis, "Real-Time Image Segmentation for Image-Guided Surgery," in *SC 1998: High Performance Networking and Computing Conference; 1998 Nov 7–13; Orlando, USA*, pp. 1114:1–14, IEEE, 1998.
28. W. Schroeder, K. Martin, and B. Lorensen, *The Visualization Toolkit: An Object-Oriented Approach to 3D Graphics*. Prentice Hall PTR, New Jersey, 1996.
29. B. Geiger, "Three dimensional modeling of human organs and its application to diagnosis and surgical planning," Tech. Rep. 2105, INRIA, 1993.
30. M. Ferrant, A. Nabavi, B. Macq, and S. K. Warfield, "Deformable Modeling for Characterizing Biomedical Shape Changes," in *DGCI2000: Discrete Geometry for Computer Imagery; 2000 Dec 13–15; Uppsala, Sweden* (G. Borgefors, I. Nyström, and G. Sanniti di Baja, eds.), vol. 1953 of *Lecture Notes in Computer Science*, (Heidelberg, Germany), pp. 235–248, Springer, 2000.
31. M. Ferrant, A. Nabavi, B. Macq, F. A. Jolesz, R. Kikinis, and S. K. Warfield, "Registration of 3D Intraoperative MR Images of the Brain Using a Finite Element Biomechanical Model," *IEEE Trans Med Imag*, 2001. In Press.
32. S. K. Warfield, F. Jolesz, and R. Kikinis, "A High Performance Computing Approach to the Registration of Medical Imaging Data," *Parallel Computing*, vol. 24, pp. 1345–1368, Sep 1998.

33. M. Ferrant, O. Cuisenaire, and B. Macq, "Multi-Object Segmentation of Brain Structures in 3D MRI Using a Computerized Atlas," in *SPIE Medical Imaging '99*, vol. 3661-2, pp. 986–995, 1999.
34. M. Ferrant, A. Nabavi, B. Macq, P. M. Black, F. A. Jolesz, R. Kikinis, and S. K. Warfield, "Serial Registration of Intra-operative MR Images of the Brain," *Med Image Anal*, 2001. In Press.
35. O. C. Zienkiewicz and R. L. Taylor, *The Finite Element Method: Basic Formulation and Linear Problems*. McGraw Hill Book Co., New York, 4th ed., 1994.
36. S. Balay, W. D. Gropp, L. C. McInnes, and B. F. Smith, "Efficient management of parallelism in object oriented numerical software libraries," in *Modern Software Tools in Scientific Computing* (E. Arge, A. M. Bruaset, and H. P. Langtangen, eds.), pp. 163–202, Birkhauser Press, 1997.
37. S. Balay, W. D. Gropp, L. C. McInnes, and B. F. Smith, "PETSc 2.0 users manual," Tech. Rep. ANL-95/11 - Revision 2.0.28, Argonne National Laboratory, 2000.